ANNALS of Clinical and Translational Neurology
Open Access
ANA American Neurological Association since 1875

RESEARCH ARTICLE

Blocking GluR2–GAPDH ameliorates experimental autoimmune encephalomyelitis

Dongxu Zhai[1,a], Frankie H. F. Lee[1,a], Cheryl D'Souza[2], Ping Su[1], Shouping Zhang[3], Zhengping Jia[3], Li Zhang[2,4], Albert H. C. Wong[1,5] & Fang Liu[1,5]

[1]Department of Neuroscience, Centre for Addiction and Mental Health, Toronto, Ontario, Canada, M5T 1R8
[2]Toronto General Research Institute, University Health Network, Toronto, Ontario, Canada
[3]Neuroscience & Mental Health, The Hospital for Sick Children, Toronto, Ontario, Canada
[4]Laboratory Medicine and Pathobiology, University of Toronto, Ontario, Canada
[5]Department of Psychiatry, University of Toronto, Ontario, Canada

Correspondence
Fang Liu, Department of Neuroscience, Centre for Addiction and Mental Health, Clarke Division, 250 College Street, Toronto, Ontario, Canada M5T 1R8. Tel: (416) 979-4659; Fax: (416) 979-4663; E-mail: f.liu.a@utoronto.ca

Funding Information
The work was supported by operating grants from Multiple Sclerosis Society of Canada and National Multiple Sclerosis Society (USA) (to F. Liu).

Received: 15 September 2014; Revised: 16 January 2015; Accepted: 19 January 2015

***Annals of Clinical and Translational Neurology* 2015; 2(4): 388–400**

doi: 10.1002/acn3.182

[a]These authors contributed equally to the study.

Abstract

Objective: Multiple sclerosis (MS) is the most common disabling neurological disease of young adults. The pathophysiological mechanism of MS remains largely unknown and no cure is available. Current clinical treatments for MS modulate the immune system, with the rationale that autoimmunity is at the core of MS pathophysiology. **Methods**: Experimental autoimmune encephalitis (EAE) was induced in mice with MOG35-55 and clinical scoring was performed to monitor signs of paralysis. EAE mice were injected intraperitoneally with TAT-fusion peptides daily from day 10 until day 30 after immunization, and their effects were measured at day 17 or day 30. **Results**: We report a novel target for the development of MS therapy, which aimed at blocking glutamate-mediated neurotoxicity through targeting the interaction between the AMPA (2-amino-3-(3-hydroxy-5-methyl-isoxazol-4-yl) propanoic acid) receptor and an interacting protein. We found that protein complex composed of the GluR2 subunit of AMPA receptors and GAPDH (glyceraldehyde-3-phosphate dehydrogenase) was present at significantly higher levels in postmortem tissue from MS patients and in EAE mice, an animal model for MS. Next, we developed a peptide that specifically disrupts the GluR2 -GAPDH complex. This peptide greatly improves neurological function in EAE mice, reduces neuron death, rescues demyelination, increases oligodendrocyte survival, and reduces axonal damage in the spinal cords of EAE mice. More importantly, our peptide has no direct suppressive effect on naive T-cell responses or basal neurotransmission. **Interpretation**: The GluR2 -GAPDH complex represents a novel therapeutic target for the development of medications for MS that work through a different mechanism than existing treatments.

Introduction

Multiple sclerosis (MS) is a demyelinating disease affecting the central nervous system, typically causing a progressive decline in motor and sensory function.[1,2] Patients with MS often suffer considerable morbidity as a result of blindness, paralysis, or fatigue. As the molecular etiology underlying MS is unclear, the disease remains a significant therapeutic challenge.[3] There is recent evidence that glutamate receptor-mediated excitotoxicity is involved in demyelination, axonal damage, and loss of neurons and oligodendrocytes.[4–7] Both NMDA (*N*-methyl-D-aspartate) receptor antagonist and AMPA (2-amino-3-(3-hydroxy-5-methyl-isoxazol-4-yl) propanoic acid)/kainite receptor antagonists NBQX or MPQX have been shown to be effective in revising neurological deficits in experimental autoimmune encephalitis (EAE) models for MS.[8–10] Unfortunately, complete glutamate receptor blockade is not a feasible clinical treatment for MS because glutamate receptors are critical for normal brain function. Noncompetitive low-affinity

antagonists such as memantine have neuroprotective effects in animal models, but worsen MS symptoms in human clinical trials.[11] Thus, our main goal was to develop a MS treatment capable of selectively blocking AMPA receptor-mediated toxicity, without interfering with other AMPA receptor-mediated physiological functions.

We chose to target the interaction between the GluR2 subunit of the AMPA glutamate receptor and GAPDH (glyceraldehyde-3-phosphate dehydrogenase) because we have shown previously that GluR2–GAPDH complex formation will lead to the activation of the p53-dependent cell death pathway upon agonist stimulation,[12] which is responsible for AMPA receptor-mediated toxicity. Furthermore, we developed a peptide (G-Gpep) that can disrupt the GluR2–GAPDH interaction that protects hippocampal neurons from AMPA receptor-mediated cell death.[13] Thus, in this article, we sought to determine whether the GluR2–GAPDH complex is involved in the pathophysiology of MS. We used two main experimental approaches: the first was to test whether the GluR2–GAPDH complex is altered in postmortem tissue from MS patients and an animal model of MS. The second was to test the efficacy of our peptide in reversing neurological deficits in rodent EAE models of MS. Our results will not only provide new insights into the pathophysiology of MS but also represents a new target for MS treatment that utilizes a novel mechanistic pathway.

Materials and Methods

Induction of chronic relapsing EAE and neurological assessment

Female C57BL/6 mice (8–12 weeks of age) were purchased from Charles River Laboratories. Mice were injected subcutaneously (s.c.) in the back with 200 μL of recombinant MOG_{35-55} (200 μg, Biomatik Corporation, Cambridge, ON, Canada), which was emulsified in incomplete Freund's adjuvant (Sigma, Oakville, ON, Canada) and supplemented with 4 mg/mL *Mycobacterium tuberculosis* (strain H37Ra, BD Biosciences, Missisauga, ON, Canada) in four different sites (50 μL per site). Two hundred nanograms of pertussis toxin (List Biological Laboratories, Inc., Campbell, CA, USA) was injected intraperitoneally (i.p.) on days 0 and 2 after immunization. Mice were assessed daily for clinical signs of disease starting on the day of immunization. Clinical scoring was performed according to the following criteria: 0, asymptomatic; 0.5, distal paresis of the tail; 1, complete tail paralysis; 1.5, paresis of the tail and mild hind limb paresis; 2, unilateral severe hind limb paresis; 2.5, bilateral severe hind limb paresis; 3, complete bilateral hind limb paralysis; 3.5 complete bilateral hind limb paralysis and paresis of one front limb; 4, complete paralysis (tetraplegia). All animal procedures used were in accordance with the approved Centre for Addiction and Mental Health animal research ethics committee protocol.

Mouse spinal cord section preparation

Lumbosacral spinal cord regions from at least three mice per group were dissected and analyzed. We selected this part of the spinal cord based on previous publications that reported distinct anatomical deficits,[14–16] and because the EAE mouse model exhibits paralysis of the hind limbs, which are under the control of the lumbar nerves. Mouse spinal cord samples from different groups were dissected after ~20 days of treatment, fixed in 4% paraformaldehyde overnight at 4°C, cryoprotected in 30% sucrose, and frozen at −80°C for future experiments. Frozen sections of 10 μm thickness were cut using a microtome cryostat system (Bright Instrument Co. 5030, Huntington, UK). Slices were then either placed in plates as free-floating sections for immunohistochemistry or on slides for Luxol Fast Blue staining.

Immunohistochemistry

Free-floating sections were initially incubated in blocking solution (0.1 mol/L phosphate-buffered saline [PBS], 5% serum, 1% Triton X-100, 0.5% Tween 20, 2% skim milk) for 1 h at room temperature to reduce nonspecific background, and then with primary and secondary antibodies overnight at 4°C. The following primary antibodies were used: anti-NeuN (1:200, Millipore, Etobicoke, ON, Canada), anti-Neurofilament-H (1:200, Abcam, Toronto, ON, Canada) and anti-CNPase (1:200, Sigma, Oakville, ON, Canada). Fluorescent secondary antibodies conjugated to Alexa 488 (Life Technologies, Burlington, ON, Canada) were used for detection of primary antibodies.

Luxol fast blue

Frozen sections on slides were placed in Luxol Fast Blue solution at 56°C overnight, differentiated with lithium carbonate and 70% ethanol until the white and gray matter are sharply defined. Cresyl violet was used as a counterstain and the slides were further dehydrated in 95% ethanol, 100% ethanol and xylene.

Quantification of neuropathology

All immunohistochemistry images of spinal cord sections were captured using a confocal microscope (Zeiss LSM510 Meta, Toronto, ON, Canada) at 10× magnification for NeuN, and 25× for neurofilament-H and

Table 1. Demographic information for multiple sclerosis (MS) specimens.

#	Age	Gender	Neuropathology diagnosis	Autolysis (T)
P1	47	F	2° Progressive MS, chronic MS plaque formation	22.1
P2	63	F	MS, chronic active MS plaque formation	21.1
P3	62	M	MS, chronic MS plaque formation	16.1
P4	64	F	2° progressive MS	7.8
P5	52	F	MS, chronic MS plaque formation	13.1
P6	62	F	MS	11.8
P7	50	F	MS	18.9
P8	67	F	MS, atherosclerosis, moderate, cerebral, chronic MS plaque formation	18.8

CNPase. Images were converted to gray values and normalized to background staining. Regions of interest (ROIs) were consistently positioned over the same analyzed region of spinal cord sections for each immunohistochemistry marker as sampling windows. A two-dimensional random sampling approach was used to provide accurate estimates of cell densities and fluorescence occupancies. We chose at least four spinal cord sections from rostral to caudal lumbar regions, and both halves of each section were used for analysis. Specific procedures for defining areas of analysis were delineated based on previous reports of histological deficits in EAE mice, and differed for each antibody as each was chosen to examine different parameters. These procedures are described in detail later.

NeuN-labeled images were used to analyze overall neuron numbers in the spinal cord gray matter. Three fixed ROIs ($225 \times 300\ \mu m^2$) were placed separately over the dorsal, intermediate, and ventral horns for each section. Fluorescently labeled cells were counted using the ITCN plugin for ImageJ (http://rsb.info.nih.gov/ij/), set with consistent parameters of width, minimum distance, and threshold. Total neuron numbers were calculated as the sum of all three ROIs. For both CNPase-stained images, two square ROIs ($50 \times 50\ \mu m^2$) were positioned near the dorsal and ventral funiculus for each spinal cord section. A similar cell counting method as described previously was used with the ITCN plugin.

For neurofilament-H, two fixed square ROIs ($200 \times 200\ \mu m^2$) were positioned over both the dorsal and ventral funiculus for analysis. Quantification of neurofilament-H was measured as the percentage of area occupied by neurofilament-H-labeling in each region. Using ImageJ, fluorescent images were converted to a black and white threshold scale, in which fluorescent colors that reaches a standard threshold become black while the rest remain white. Hence, calculating the black area per total area represents fluorescence occupancy.

Finally, Luxol Fast Blue images at 4× magnification were captured under brightfield illumination with a Nikon Eclipse E600 microscope (Melville, NY, USA). Likewise, two fixed square regions ($300 \times 300\ \mu m^2$) were placed over both the dorsal and ventral funiculus. Images were converted to gray scale and calculated according to precalibrated values of optical density in black and white transmission. Myelin density was then measured in optical density within each ROI. Acquisition parameters were kept the same for all images.

Statistical analysis of neuropathology

Student's two-tailed *t*-test was performed in comparing between each treatment group with either sham or TAT-G-Gpep-treated group. Data are expressed as mean ± standard error of mean (SEM). A significance level of $P < 0.05$ was used for all analyses.

Co-immunoprecipiation and western blot analysis

Co-immunoprecipitation and western blot analyses were performed using postmortem human tissue or mouse lumbar spinal cord tissue (100 mg). We used eight postmortem brain tissues from healthy people as control, eight postmortem plaque brain tissues and eight cervical cord tissues from MS patients. For co-immunoprecipitation and western blot analysis with mouse tissue, we used three tissue samples for each group. Protein was extracted in buffer containing (in mmol/L): 50 Tris-Cl, pH 7.4, 150 NaCl, 2 EDTA, 1 PMSF plus 1% Igepal CA-630, 0.5–1% sodium deoxycholate, 1% Triton X-100 and protease inhibitor mixture (5 μL/100 mg of tissue; Sigma). For co-immunoprecipitation experiments, solubilized spinal cord protein (500–700 μg) was incubated in the presence of primary antibodies anti-GluR2 (Novus Biologicals, Oakville, ON, Canada), or rabbit IgG (2–4 μg) for 3 h at 4°C, followed by the addition of 25 μL of protein A/G plus agarose (Santa Cruz Biotechnology, Santa Cruz, CA) for 12 h before subjecting to SDS-PAGE (sodium dodecyl sulfate polyacrylamide gel electrophoresis) for western blot analysis. Besides, we detected the expression level of GluR2 and GAPDH using SDS-PAGE and western blot

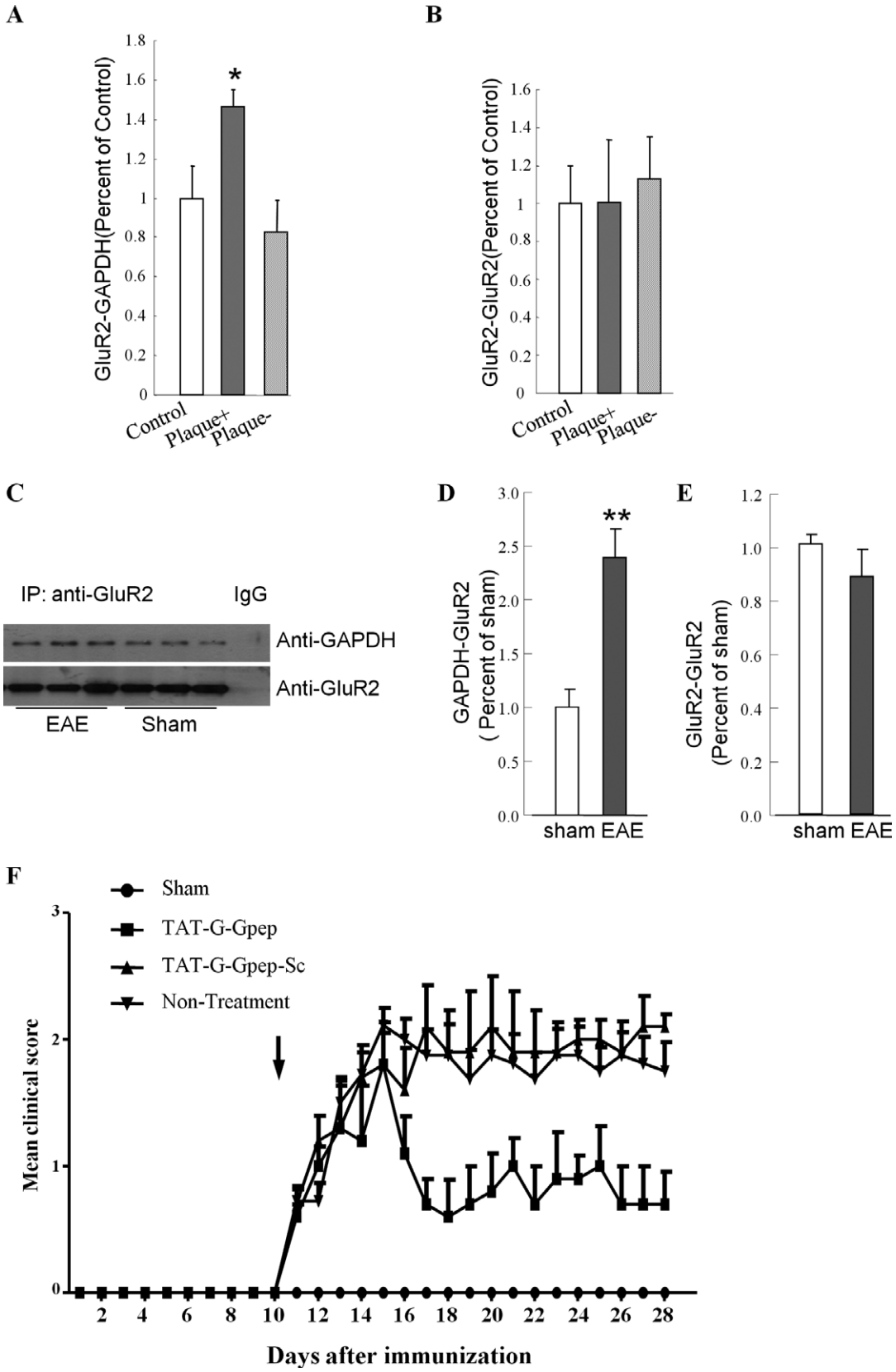

Figure 1. GluR2–GAPDH complex in multiple sclerosis (MS). (A, B) GluR2–GAPDH complex formation is significantly increased in the plaque of multiple sclerosis (MS). Postmortem samples from control, MS plaque (plaque+) area, and MS nonplaque (plaque−) area were incubated with GluR2 antibody and the precipitated proteins were immunoblotted with GAPDH antibody or GluR2 antibody. The intensity of each protein band for GAPDH (A), GluR2 (B) from all three groups was quantified by densitometry (AIS software, Imaging Research Inc.). Results for each sample are presented as the percentage of the mean of the control samples on the same blot. (*$P < 0.05$, $n = 8$, one-way ANOVA). (C–E) GluR2–GAPDH complex formation is significantly increased in experimental autoimmune encephalitis (EAE) mice compared to sham mice. (A) Representative image of western blot analysis of GAPDH (top) and GluR2 (bottom) levels precipitated by GluR2 antibody in extract prepared from mouse spinal cord tissue were incubated with GluR2 antibody. Precipitated proteins were subject to SDS-PAGE (sodium dodecyl sulfate polyacrylamide gel electrophoresis) and immunoblotted with GAPDH or GluR2 antibody. (D, E) Densitometric analysis of the level of GAPDH and GluR2. The intensity of GAPDH and GluR2 was quantified by densitometry (software: Image J, NIH). Data were analyzed by *t*-test. (**$P < 0.01$, $n = 3$). (F) Clinical EAE scores (mean ± SEM) over time of four groups vaccinated with MOG_{35-55} on day 0 and treated intraperitoneally daily with TAT-G-Gpep and TAT-G-Gpep-Sc from day 10 (arrow). Starting from day 12, $P < 0.05$, data were analyzed by Mann–Whitney *U* test.

analysis with 50 μg protein extract of every sample from either human tissue or mouse tissue. When doing the SDS-PAGE with samples of postmortem human tissue, we loaded four samples from control group with the samples from either plaque or cervical cord tissue group. For experiments with mouse tissue, we loaded all 12 samples from the four groups on the same gel. Blots were blocked for 1 h before incubating with the appropriate primary antibody (anti-GAPDH, mouse, Millipore; anti-GluR2, rabbit, Millipore; anti-Neurofilament-H, mouse, Millipore) overnight at 4°C. The membrane was incubated with horseradish peroxidase-conjugated secondary antibody (diluted in 1% bovine serum albumin in Tris-Buffered Saline in Tween 20; Sigma, Oakville, ON, Canada) for 1.5 h at room temperature. The proteins were visualized with enhanced chemiluminescence reagents as described (Amersham Biosciences, Buckinghamshire, UK).

T-cell recall response

Draining lymph nodes were harvested from mice and single-cell preparations were obtained by passage through 40 μmol/L nylon cell strainers (BD Falcon, Mississauga, ON, Canada). Red blood cells were lysed in lysis buffer (0.14 mol/L ammonium chloride, 0.02 mol/L Tris, pH 7.2). Cells were labeled with 1 μmol/L carboxyfluorescein succinimidyl ester CFSE (Life Technologies, Burlington, ON, Canada) as per manufacturer's instructions and cultured in 96-well plates (0.5×10^6/well) in RPMI containing 10% fetal bovine serum FBS (Life Technologies, Burlington, ON, Canada) with 10 μg/mL MOG for 3 days. Cells were then collected and stained for flow cytometry. Supernatants were frozen for cytokine analysis.

Bio-plex assay for interferon-γ and interleukin-17

The bioplex assay was performed according to the manufacture's instruction (#L60-00004C6, Bio-Rad Laboratories, Inc., Mississauga, ON, Canada). Briefly, samples were thawed at room temperature and incubated with antibody microbeads for 30 min. After rinsing, the beads were incubated with the detection antibody cocktail, followed by streptavidin–phycoerythrin for 10 min. Finally, the concentration of each cytokine was determined by the Bio-Plex Suspension Array Reader.

Preparation of mouse splenocyte cultures

Spleens were harvested from C57BL/6 mice (Charles Rivers, Senneville, QC, Canada) and single-cell preparations were obtained by passage through 40 μmol/L nylon cell strainers (BD Falcon). Red blood cells were lysed in Lysis Buffer (0.14 mol/L ammonium chloride, 0.02 mol/L Tris, pH 7.2). Cells were labeled with 1 μmol/L CFSE (Life Technologies) as per manufacturer's instructions and cultured in six-well plates (1.6×10^7/well, BD Falcon) in RPMI containing 10% FBS (Gibco) with 5 μg/mL PHA (Sigma, Canada) and various concentrations of the TAT-G-Gpep or TAT-G-Gpep-Sc for 3 days. Cells were then collected and stained for flow cytometry.

Isolation and culture of human peripheral blood mononuclear cells

Human peripheral blood mononuclear cells (PBMCs) were isolated from the blood obtained from consenting healthy donors. Blood was collected in Sodium Heparin BD Vacutainer tubes and diluted 1:1 in PBS containing 2% FBS. The mixture was overlayed onto 15 mL Ficoll-Paque (GE Healthcare, Baie d'Urfe, QC, Canada) in SepMate tubes (Stemcell Technologies, Vancouver, BC, Canada) and spun at 1200*g* for 20 min. The buffy coat containing the PBMCs was collected and washed twice with PBS containing 2% FBS. Cells were counted on a Vi-CELL cell counter (Beckman Coulter, Mississauga, ON, Canada).

PBMCs were labeled with 1 μmol/L CFSE (Life Technologies) as per manufacturer's instructions and cultured

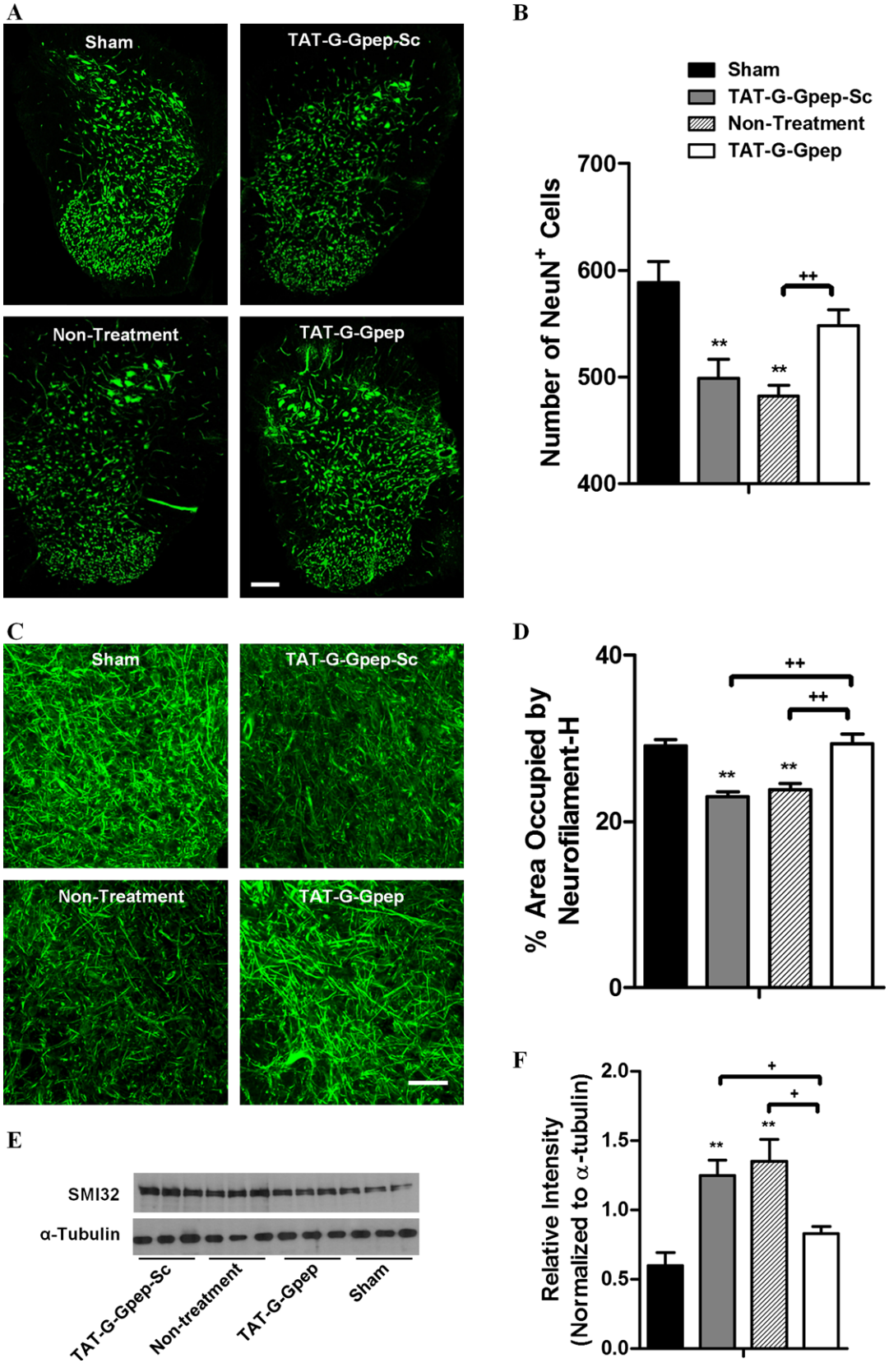

Figure 2. TAT-G-Gpep treatment rescues both neuronal and axonal density in mouse spinal cords with experimental autoimmune encephalitis (EAE). (A) Representative images of mouse spinal cords immunostained against $NeuN^+$ in sham, TAT-G-Gpep-Sc, nontreatment and TAT-G-Gpep treatment groups. Scale bar = 100 μm. (B) There was a significantly fewer total number of neurons in Tat-G-Gpep-Sc and nontreatment groups when compared to sham animals. However, TAT-G-Gpep treatment resulted in a significant increase in $NeuN^+$ cells versus nontreatment mice, and was comparable to sham controls. There was also an increasing trend observed with TAT-G-Gpep treatment when compared to TAT-G-Gpep-Sc group. (C) Neurofilament-H immunostained images of mouse spinal cords in sham, TAT-G-Gpep-Sc, nontreatment and TAT-G-Gpep treatment groups. Scale bar = 15 μm. (D) Quantification of neurofilament-H staining was converted to a black and white threshold scale and expressed as a percentage of area occupied by fluorescence in the dorsal and ventral funiculi of mouse spinal cords. The area occupied by neurofilament-H labeling was significantly lower in TAT-G-Gpep-Sc and nontreated mice when compared to sham, while TAT-G-Gpep-treated mice showed a significant rescue in axon density which was comparable to sham controls. All data are shown as mean ± SEM; $*P < 0.05$, $**P < 0.01$ versus sham; $++P < 0.01$. (E) Axonal damage, assessed by western blot for abnormally dephosphorylated neurofilament-H. Western blot analysis of whole spinal cord homogenate, visualized by enhanced chemiluminescent ECL, of proteins from all four groups: sham, TAT-G-Gpep-Sc, nontreatment and TAT-G-Gpep treatment groups. (F) Densitometric analysis of western blots of total spinal cord homogenate of three representative mice per group, developed by horseradish peroxidase/3, 3′-diaminobenzidine HRP/DAB. Data represent means ± SEM. Differences between groups were accessed by Student–Newman–Keuls post hoc one-way ANOVA $**P < 0.01$ versus sham controls, $+P < 0.05$.

in 96-well flat-bottom plates (10^5/well) coated with 5 μg/mL anti-CD3 mAb (OKT3, eBioscience, San Diego, CA, USA) in RPMI containing 10% FBS (Life Technologies) and 250 IU/mL recombinant human IL-2 (Proleukin, Chiron Corporation, Emeryville, CA, USA). TAT-G-Gpep, TAT-G-Gpep-Sc, or IFN-β (Bio Basic Inc., Markham, ON, Canada) were added to the wells and cultured for 3 days. Cells were subsequently harvested and stained for flow cytometry.

Flow cytometry

Antibodies used for flow cytometry include: mouse anti-CD4 (GK1.5), anti-CD8 (53-6.7), anti-CD25 (PC61), anti-CD69 (HI.2F3), all from Biolegend, as well as human anti-CD4 (OKT4), anti-CD8 (HIT8a), anti-CD25 (BC96), all from Biolegend and anti-CD69 (FN50) from eBioscience. Cells were also stained with either 7-AAD (Sigma, Oakville, ON, Canada) or eFluor450 (eBioscience) to identify dead cells. Data were acquired using an Accuri C6 (BD Biosciences) and an LSRII (BD Biosciences) cytometer and analyzed with FlowJo software (TreeStar).

Electrophysiology

The procedures for electrophysiological recordings were described previously.[14–16] Briefly, hippocampal slices (400 μm) were prepared from 6- to 7-week-old mice injected with active or scrambled control peptides as described for behavioral and biochemical assessment, and allowed to recover in a holding chamber for at least 2 h. A single slice was then transferred to the recording chamber, submerged and superfused with 95% O_2– 5% CO_2 saturated artificial cerebrospinal fluid (ACSF, 2 mL/min), which contained (in mmol/L)120 NaCl, 2.5 KCl, 1.3 $MgSO_4$, 1.0 NaH_2PO_4, 26 $NaHCO_3$, 2.5 $CaCl_2$, and 11 D-glucose. The recording pipette (3 MΩ) was filled with ACSF solution. Synaptic responses at the CA1 synapse were evoked by bipolar tungsten electrodes placed 50–100 μm from the cell body layer in the CA1 area. The distance between recording and stimulating electrodes were kept constant between slices. Field excitatory postsynaptic potentials (fEPSPs) were measured by taking the slope of the rising phase between 5% and 60% of the peak response. All data acquisition and analysis were done using pCLAMP 8 software (Molecular Devices, Sunnyvale, CA, USA) and were statistically evaluated by Student's *t*-test.

Peptides

The specific peptide used in this study has been reported previously.[13] All peptides were synthesized and purchased from Biomatik Corporation (Cambridge, USA). Both the $GluR2_{NT1\text{-}3\text{-}2}$ peptide and scrambled $GluR2_{NT1\text{-}3\text{-}2}$ peptide were fused to the cell membrane transduction domain of the HIV-1 TAT peptide [YGRKKRRQRRR] to facilitate the intracellular delivery. The sequence for TAT-G-Gpep was YGRKKRRQRRRYYQWDKFAYLYDSDRGLSTLQA V LDSAAEK, and the sequence for TAT-G-Gpep-Sc is YGRKKRRQRRR AFDLSQYDLKWQVDYLKYDYGTASEL RASA. The peptide was purified by high-performance liquid chromatography, with purity of at least 90%, dissolved in saline and aliquoted accordingly prior to use and stored at −80°C.

Statistical analysis of EAE clinical score

The statistics of the EAE clinical score was analyzed with the Mann–Whitney *U* test, while other experiments were analyzed by one-way analysis of variance (ANOVA) followed by post hoc Student–Newman–Keuls test or Student's *t*-test. Statistical significance was achieved when $P < 0.05$.

Results and Discussion

We initiated our investigation with co-immunoprecipitation experiments, using a primary antibody against GluR2, on 16 postmortem spinal cord samples from the Human Brain and Spinal Fluid Resource Center (HBSFRC), University of California, Los Angeles. There were samples from eight unaffected controls and eight MS patients. Demographic information for the MS specimens including the type of MS, age, sex, and autolysis time is shown in Table 1. For each MS sample, two areas were tested: MS plaques and normal cervical spinal cord, for a total of 24 samples. The same amount of protein from each sample was incubated with anti-GluR2 antibody and protein A/G agarose. The precipitated proteins were divided equally into two groups before being subjected to SDS-PAGE and immunoblotted with either GAPDH antibody or GluR2 antibody.

As shown in Figure 1A, co-immunoprecipitation of GAPDH by the GluR2 antibody was significantly greater in protein extracted from MS spinal cord plaques compared to both healthy regions spinal cord from MS patients and healthy control subjects ($n = 8$, $P < 0.05$). In contrast, neither the levels of directly immunoprecipitated GluR2 (Fig. 1B) nor the expression of GluR2 and GAPDH was significantly different between all groups (Fig. S1A and B). These data suggest an increased level of GluR2–GAPDH complex in MS plaques but not healthy tissue.

The increased GluR2–GAPDH interaction in MS patients also suggests that disruption of GluR2–GAPDH coupling might be therapeutic for MS. We chose EAE mice to test the effect of our interfering peptide because it is the most commonly used experimental model for MS. EAE is a complex syndrome in which the interactions between a variety of immunopathological and neuropathological mechanisms lead to an approximation of the key pathological features of MS: inflammation, demyelination, axonal loss, and gliosis.[17,18]

EAE mice were induced using MOG_{35-55} emulsified with CFA as described previously.[19] The mice were observed daily for signs of gait and motor dysfunction (details described in Materials and Methods section), which was used as a clinically relevant indicator of the typical effects of demyelination in the spinal cord.[17] At day 10 after immunization, the mice started to develop MS-like symptoms as reflected by the daily increase in the rating of motor dysfunction, which is consistent with previous reports.[20] Mice were treated daily (i.p.) with either TAT-G-Gpep or the scrambled amino acid sequence control peptide TAT-G-Gpep-Sc, from day 10 until day 28. As shown in Figure 1C–E, EAE mice displayed increased GluR2–GAPDH co-immunoprecipitation ($n = 3$, t-test $P < 0.01$; mean $\pm$ SEM). There was no difference in directly immunoprecipitated GluR2 between the two groups. These data demonstrate an increased GluR2–GAPDH interaction in both MS patients and EAE mice, and suggest that disrupting this interaction with TAT-G-Gpep may have therapeutic benefits in MS.

To test this hypothesis, we examined the effect of TAT-G-Gpep treatment on motor dysfunction in EAE mice. As shown in Figure 1F and the Video S1, TAT-G-Gpep treatment significantly improved motor function (quantified as the "clinical score") compared to control peptide treatment. There was no significant difference between control peptide-treated EAE mice and saline-treated EAE mice. The dramatic improvement in the EAE mice after TAT-G-Gpep treatment was best appreciated by viewing the Video S1, in which the hind limb paralysis was significantly improved. These data indicate that disruption of the GluR2–GAPDH interaction may be able to reverse the clinical symptoms of MS.

Loss of myelin, oligodendrocytes, and some axons are core features of MS pathology. Previous studies have shown that AMPA receptor antagonists can ameliorate autoimmune encephalomyelitis, by promoting neuron, oligodendrocyte, and axon survival, and rescuing demyelination in the spinal cords of EAE rats and mice.[8–10] We have shown previously that disruption of the GluR2–GAPDH interaction can block AMPA receptor-mediated neurotoxicity.[12,13,21] To determine whether disruption of GluR2–GAPDH interaction has protective effects in EAE mice, we examined lumbar spinal cord sections from EAE mice treated with TAT-G-Gpep peptide in comparison to control peptide. We initially assessed whether TAT-G-Gpep treatment would alter neuronal density in lumbar spinal cord from EAE mice using an antibody against NeuN. NeuN-positive cells were counted in fixed regions of interest positioned over the dorsal, intermediate, and ventral zones of spinal gray matter. As shown in Figure 2A and B, EAE mice without peptide treatment and with control peptide treatment displayed a significant loss of spinal cord neurons when compared to sham controls. However, EAE mice treated with TAT-G-Gpep had significantly higher neuronal numbers that were comparable to sham (non-EAE) mice.

Next, we examined axonal integrity in our treatment groups with an antibody that recognizes a phosphorylated epitope of neurofilament-H. As shown in Figure 2C and D, there was substantial axonal damage present in EAE mouse spinal cord compared to sham animals. Significantly less axonal damage was seen with TAT-G-Gpep treatment. Consistent results were obtained from western blot analysis using an antibody that recognizes dephosphorylated neurofilament-H (SMI32) (Fig. 2E and F). These results suggest that blocking the interaction

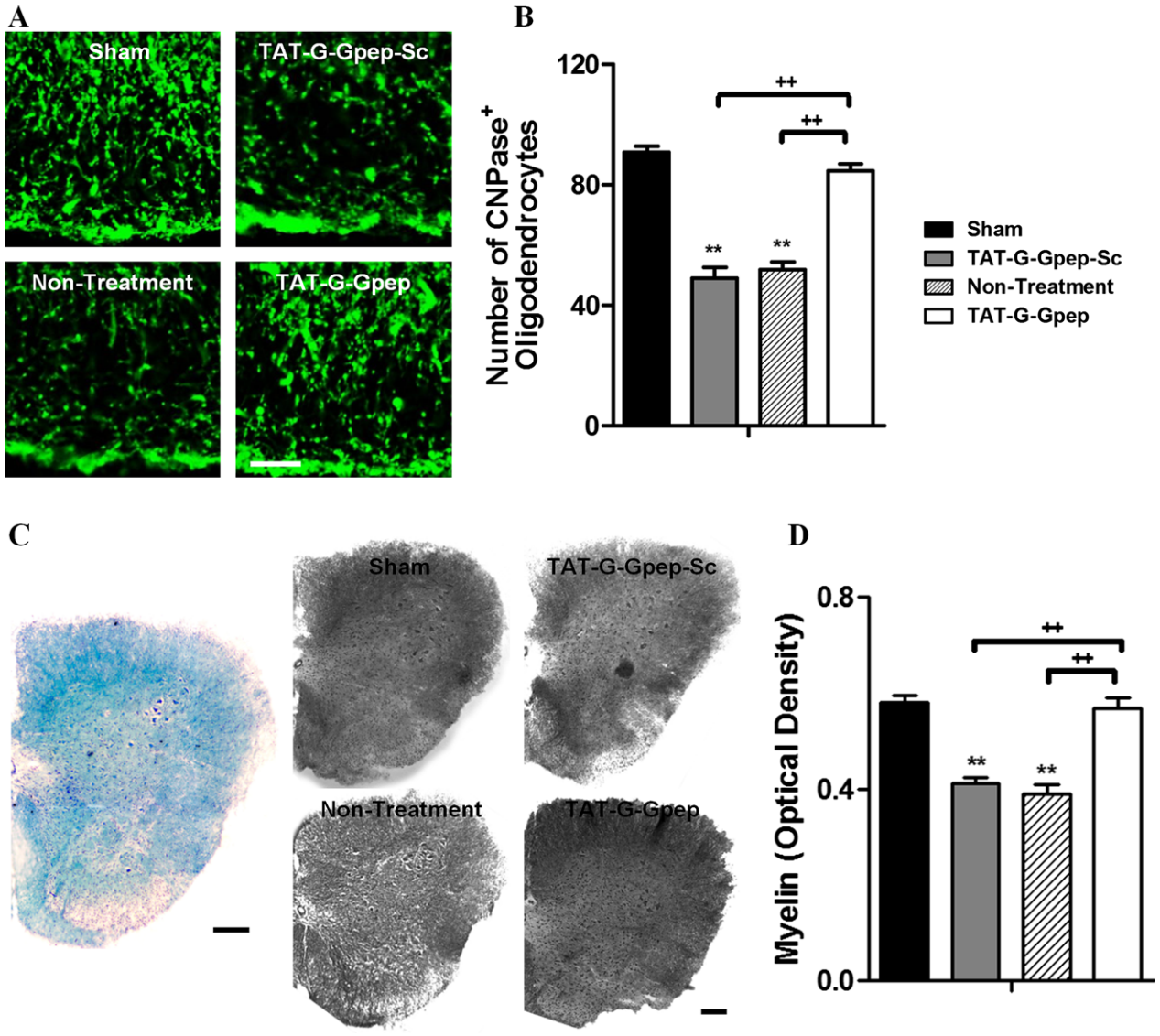

Figure 3. Administration of TAT-G-Gpep significantly promotes oligodendrocyte survival and rescues demyelination in the experimental autoimmune encephalitis (EAE) mouse spinal cords. (A) Representative images of fluorescently labeled CNPase-reactive oligodendrocytes in sham, TAT-G-Gpep-Sc, nontreated, and TAT-G-Gpep-treated mouse spinal cords. Scale bar = 15 μm. (B) There were significantly fewer CNPase-immunolabeled oligodendrocytes in TAT-G-Gpep-Sc and nontreated mice when compared to sham. But TAT-G-Gpep treatment significantly rescued oligodendrocyte numbers to a level comparable to sham controls. (C) Representative Luxol Fast Blue image of an EAE mouse spinal cord section with no treatment is shown in blue. Luxol Fast Blue staining was used to quantify myelination (blue) in different groups. Color images converted to gray scale values of the four groups are shown on the right. Scale bar = 100 μm. (D) Myelin density was measured as optical density according to precalibrated values in black and white transmission. Similarly, significant demyelination was observed in TAT-G-Gpep-Sc and nontreated mice when compared to sham. TAT-G-Gpep treatment significantly increased myelination to sham control levels. All data are shown as mean ± SEM; $^{**}P < 0.01$ versus sham, $^{++}P < 0.01$.

between GluR2 subunit and GAPDH with TAT-G-Gpep can rescue neuronal death and axon damage.

Axonal loss in MS is commonly believed to be a consequence of myelin damage.[22] Indeed, a pathological hallmark of MS is the demyelination of axons and death of oligodendrocytes, which are the main cells responsible for myelin production. Since we showed that TAT-G-Gpep can reduce axonal damage, we then investigated whether the protective effect of the TAT-G-Gpep peptide resulted from promoting oligodendrocyte survival and preventing axon demyelination.

Immunohistochemistry using antibodies against CNPase was used to detect oligodendrocytes in spinal cord sections from different treatment groups. As shown

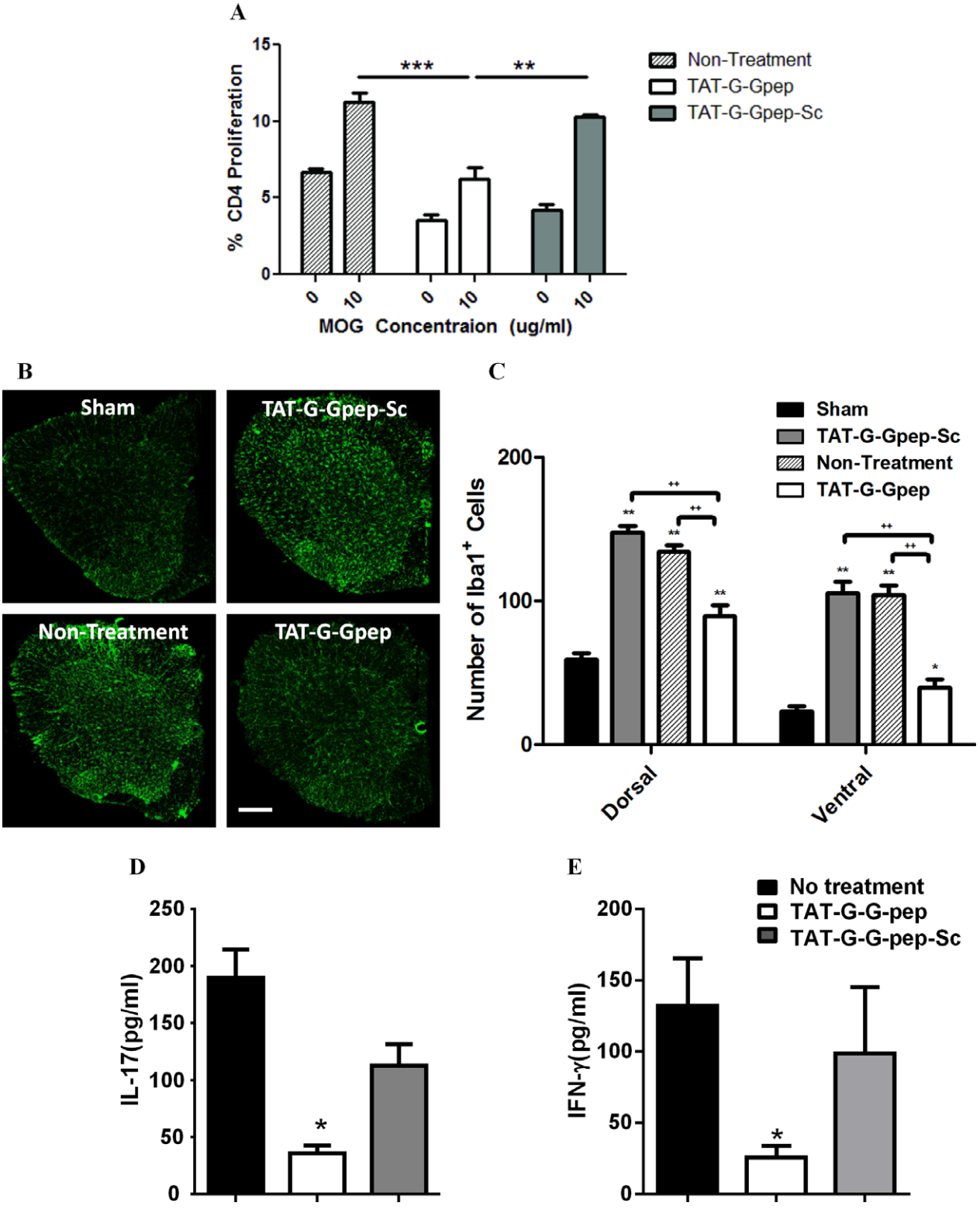

Figure 4. TAT-G-Gpep treatment diminishes the activated immune response in experimental autoimmune encephalitis (EAE) mice. (A) EAE mice in all groups showed an increase in $CD4^+$ T-cell proliferation when presented with 10 μg/mL of MOG. TAT-G-Gpep administration significantly reduced this proliferative response. $^{**}P < 0.01$; $^{***}P < 0.001$. (B) Representative images of Iba1-immunolabeled macrophages/microglia in sham, TAT-G-Gpep-Sc, nontreated and TAT-G-Gpep-treated mouse spinal cords. Scale bar = 100 μm. (C) Quantification of the number of $Iba1^+$ cells in the dorsal and ventral horns revealed significantly more macrophages/microglia residing in scrambled peptide, nontreated and peptide-treated mice when compared to sham. Peptide treatment significantly reduced the amount $Iba1^+$ cells when compared to scrambled peptide or nontreated mice. All data are shown as mean ± SEM; $^{**}P < 0.01$ versus sham; $^{+}P < 0.01$. (D, E) TAT-G-Gpep treatment in EAE mice resulted in a significant reduction in IL-17 (D) and IFN-γ (E) levels when compared to nontreated or TAT-G-Gpep-Sc treated mice. $^{*}P < 0.05$.

in Figure 3A and B, the number of CNPase-positive oligodendrocytes was significantly lower in the EAE group without treatment and with control peptide treatment compared to sham. However, the decreased oligodendrocyte numbers were restored to almost normal sham levels after TAT-G-Gpep treatment, suggesting that disruption of the GluR2 and GAPDH interaction can promote oligodendrocyte survival.

Using Luxol Fast Blue staining, we also analyzed the effects of TAT-G-Gpep treatment on myelin. As shown in Figure 3C and D, untreated EAE mice or those treated with control peptide treatment had a significant reduction in myelin when compared to sham animals. However, myelination was restored to control levels with TAT-G-Gpep treatment. Collectively, our results indicate that the GluR2–GAPDH interaction is critical in modulating oligodendrocyte number and myelin production in an animal model of MS. Our results also suggest that our interfering peptide can repair the histopathological damage in MS, in addition to restoring neurological function.

EAE has been regarded as a primarily $CD4^+$ T-cell-mediated condition. Current clinical treatment for MS targets the inflammatory process through immunosuppression.[2,23,24] Thus, it is important to determine the effects of the TAT-G-Gpep peptide on $CD4^+$ T-cell activation and proliferation. We first determined the effects of the TAT-G-Gpep peptide on the immune system of EAE mice *in vivo* using T-cell recall response assays. Since we showed that the motor function of EAE mice treated with TAT-G-Gpep peptide improved considerably by day 17 after immunization (Fig. 1F), we examined $CD4^+$ T-cell proliferation in draining lymph node cells of EAE mice at that time. Cells were CFSE-labeled and restimulated with MOG_{35-55} *in vitro* for 3 days. As seen in Figure 4A, $CD4^+$ T-cells from EAE mice without treatment or treated with control peptide proliferated vigorously upon MOG_{35-55} restimulation. In contrast, $CD4^+$ T-cells from EAE mice treated with TAT-G-Gpep had a significantly reduced proliferative response to MOG_{35-55} restimulation, suggesting that TAT-G-Gpep can dampen an already activated immune response. As MS is closely associated with inflammation, we then tested whether TAT-G-Gpep affects microglial/macrophage recruitment on mouse spinal cord sections against ionized calcium-binding adapter molecule 1 Iba1 in all groups and quantified Iba1-immunolabeled microglia/macrophages in the dorsal and ventral horn regions. As shown in Figure 4B and C, the number of $Iba1^+$ cells was significantly increased in EAE mice without treatment or treated with control peptide when compare to sham group, while TAT-G-Gpep administration significantly decreased Iba1-cells in EAE mice. Consistent with this, levels of both IFN-γ and IL-17, two key proinflammatory cytokines involved in the pathogenesis of EAE, were reduced in supernatants of EAE mice treated with TAT-G-G peptide. Levels in supernatants from EAE mice treated with control peptide were similar to those from untreated EAE mice. These results reinforce our finding that TAT-G-Gpep is able to modulate the inflammatory response in the EAE model.

Next, we examined whether the observed inhibitory effect of TAT-G-Gpep on $CD4^+$ T-cell proliferation is a result of direct immunosuppression of these T-cells. To this end, mouse splenocytes were cultured *in vitro* with varying concentrations of TAT-G-Gpep during PHA (phytohemagglutinin)-induced activation and proliferation. As shown in Figure S2, there was a strong proliferative response when cells were incubated with PHA (positive control) compared to those incubated without PHA (negative control). $CD4^+$ T-cells treated with TAT-G-Gpep or control peptide showed just as strong a proliferative response as the positive control. To determine whether TAT-G-Gpep peptide had more subtle effects on $CD4^+$ T-cell activation, we examined the expression of activation markers after mouse splenocytes were activated in the presence or absence of peptides. Again, the level of expression of CD25 and CD69 on $CD4^+$ T-cells incubated with either TAT-G-Gpep or control peptide at various concentrations was comparable to that of the positive control (Fig. S3).

To further investigate the effects of TAT-G-Gpep peptide on human T-cells, human PBMCs were cultured in the presence or absence of control peptide or TAT-G-Gpep. $CD4^+$ and $CD8^+$ T-cell proliferation was then examined after 3 days of anti-CD3 stimulation. We used IFN-β, a common medication for clinical treatment of MS, as a positive control. As shown in Figure S4A and B, similar to what was observed for mouse $CD4^+$ T-cells, the

addition of the TAT-G-Gpep or control peptide to human PBMC cultures had no effect on the proliferative response of $CD4^+$ or $CD8^+$ T-cells, while IFN-β significantly inhibited both $CD4^+$ and $CD8^+$ T-cell proliferation (Fig. S4C and D). Collectively, these data indicate that TAT-G-Gpep has no direct effect on primary mouse or human T-cell activation or proliferation *in vitro*.

Although neuroprotective effects of NMDA and AMPA receptor antagonists have consistently been demonstrated in numerous animal models of diseases such as stroke and MS,[8–10,25] clinical use of these antagonist-based neuroprotective therapies is limited by the critical role of NMDA and AMPA receptors in excitotoxicity and excitatory neurotransmission.[26] Thus, our promising results showing that TAT-G-Gpep can improve neurological function and protect myelin, oligodendrocytes, and axons would not be clinically useful if TAT-G-Gpep blocks AMPA receptor-mediated neurotransmission.

To determine whether our peptide has any effect on synaptic transmission, we conducted electrophysiological recordings in the CA1 region of the hippocampus.[27] The mice were injected (i.p.) with TAT-G-Gpep or control peptide. fEPSPs were then recorded from hippocampal slices from these mice. As shown in Figure S5A–C, no significant differences were found in either prefiber volleys or fEPSP over a range of stimulation intensities. These results indicate that the effect of the peptide on behavior is independent of modulating synaptic transmission.

Recent evidence suggest that both AMPA receptor and NMDA receptor antagonists are effective in reducing neurological deficits in EAE models for MS.[8–10,28] Ideally, clinical treatments for MS targeting glutamate signaling should not inhibit basal neurotransmission. By blocking the interaction between AMPA receptor and GAPDH, we have developed a potential MS treatment capable of selectively inhibiting AMPA receptor-mediated toxicity, without interfering with basal neurotransmission, which is the fatal side effect of clinical application of NMDA/AMPA receptor antagonists. The GluR2–GAPDH interaction is therefore a promising new target for MS treatment that has significant potential to improve MS outcomes.

Acknowledgments

The work is supported by operating grants from Multiple Sclerosis Society of Canada and National Multiple Sclerosis Society (USA) (to F. Liu).

Conflict of Interest

None declared.

References

1. Trapp BD, Stys PK. Virtual hypoxia and chronic necrosis of demyelinated axons in multiple sclerosis. Lancet Neurol 2015;2:388–400.
2. Compston A, Coles A. Multiple sclerosis. Lancet 2008;372:1502–1517.
3. Kieseier BC, Wiendl H, Hemmer B, Hartung HP. Treatment and treatment trials in multiple sclerosis. Curr Opin Neurol 2007;20:286–293.
4. Trapp BD, Nave KA. Multiple sclerosis: an immune or neurodegenerative disorder? Annu Rev Neurosci 2008;31:247–269.
5. Stys PK, Zamponi GW, van Minnen J, Geurts JJ. Will the real multiple sclerosis please stand up? Nat Rev Neurosci 2012;13:507–514.
6. Bolton C, Paul C. Glutamate receptors in neuroinflammatory demyelinating disease. Mediators Inflamm 2006;2006:93684.
7. Newcombe J, Uddin A, Dove R, et al. Glutamate receptor expression in multiple sclerosis lesions. Brain Pathol 2008;18:52–61.
8. Basso AS, Frenkel D, Quintana FJ, et al. Reversal of axonal loss and disability in a mouse model of progressive multiple sclerosis. J Clin Investig 2008;118:1532–1543.
9. Smith T, Groom A, Zhu B, Turski L. Autoimmune encephalomyelitis ameliorated by AMPA antagonists. Nat Med 2000;6:62–66.
10. Pitt D, Werner P, Raine CS. Glutamate excitotoxicity in a model of multiple sclerosis. Nat Med 2000;6:67–70.
11. Villoslada P, Arrondo G, Sepulcre J, et al. Memantine induces reversible neurologic impairment in patients with MS. Neurology 2009;72:1630–1633.
12. Wang M, Li S, Zhang H, et al. Direct interaction between GluR2 and GAPDH regulates AMPAR-mediated excitotoxicity. Mol Brain 2012;5:13.
13. Zhai D, Li S, Wang M, et al. Disruption of the GluR2/GAPDH complex protects against ischemia-induced neuronal damage. Neurobiol Dis 2013;54:392–403.
14. Soulika AM, Lee E, McCauley E, et al. Initiation and progression of axonopathy in experimental autoimmune encephalomyelitis. J Neurosci 2009;29:14965–14979.
15. Bannerman P, Hahn A, Ramirez S, et al. Motor neuron pathology in experimental autoimmune encephalomyelitis: studies in THY1-YFP transgenic mice. Brain 2005;128:1877–1886.
16. Liu L, Huang D, Matsui M, et al. Severe disease, unaltered leukocyte migration, and reduced IFN-γ production in CXCR3−/− mice with experimental autoimmune encephalomyelitis. J Immunol 2006;176:4399–4409.
17. Lubetzki C, Williams A, Stankoff B. Promoting repair in multiple sclerosis: problems and prospects. Curr Opin Neurol 2005;18:237–244.

18. Rivers TM, Schwentker FF. Encephalomyelitis accompanied by myelin destruction experimentally produced in monkeys. J Exp Med 1935;61:689–702.
19. Miller SD, Karpus WJ, Davidson TS. Experimental autoimmune encephalomyelitis in the mouse. Current protocols in immunology 2007: 15.1. 1–.1. 20
20. Lyons JA, San M, Happ MP, Cross AH. B cells are critical to induction of experimental allergic encephalomyelitis by protein but not by a short encephalitogenic peptide. Eur J Immunol 1999;29:3432–3439.
21. Zhai D, Chin K, Wang M, Liu F. Disruption of the nuclear p53-GAPDH complex protects against ischemia-induced neuronal damage. Mol Brain 2014;7:20.
22. Bitsch A, Schuchardt J, Bunkowski S, et al. Acute axonal injury in multiple sclerosis. Correlation with demyelination and inflammation. Brain 2000;123(Pt 6):1174–1183.
23. Wingerchuk DM, Carter JL. Multiple sclerosis: current and emerging disease-modifying therapies and treatment strategies. Mayo Clin Proc 2014;89:225–240.
24. Ontaneda D, Hyland M, Cohen JA. Multiple sclerosis: new insights in pathogenesis and novel therapeutics. Annu Rev Med 2012;63:389–404.
25. Simon RP, Swan JH, Griffiths T, Meldrum BS. Blockade of *N*-methyl-D-aspartate receptors may protect against ischemic damage in the brain. Science 1984;226: 850–852.
26. Roesler R, Quevedo J, Schroder N. Is it time to conclude that NMDA antagonists have failed? Lancet Neurol 2003;2:13; discussion.
27. Meng Y, Zhang Y, Jia Z. Synaptic transmission and plasticity in the absence of AMPA glutamate receptor GluR2 and GluR3. Neuron 2003;39:163–176.
28. Kanwar JR, Kanwar RK, Krissansen GW. Simultaneous neuroprotection and blockade of inflammation reverses autoimmune encephalomyelitis. Brain 2004;127(Pt 6):1313–1331.

Supporting Information

Additional Supporting Information may be found in the online version of this article:

Figure S1. No change in GluR2 and GAPDH expression in multiple sclerosis (MS) patient samples. Densitometric analysis of western blots of the expression level of GluR2 (A) and GAPDH (B) of postmortem tissues extracted from control subjects, plaque area of MS patients, and nonplaque area of MS patients. Results for each sample are presented as the percentage of the mean of the control samples on the same blot (n = 8, one-way ANOVA).

Figure S2. TAT-G-Gpep does not affect mouse $CD4^+$ T-cell proliferation. C57BL/6 mouse splenocytes were labeled with CFSE and cultured with 5 μg/mL PHA for 3 days with TAT-G-Gpep-Sc (10 μmol/L) or varying concentrations of TAT-G-Gpep. Cells were collected and stained for CD4. (A) Representative flow cytometry plots of CFSE dilution. Negative control: no PHA, no peptide, positive control: PHA, no peptide. (B) Quantitation of % $CD4^+$ T-cell proliferation from two independent experiments.

Figure S3. Mouse activation marker expression is not affected by TAT-G-Gpep. Mouse splenocytes were cultured with PHA and TAT-G-Gpep-Sc or TAT-G-Gpep. After 3 days, cells were collected and stained for CD4, CD69, and CD25. Negative and positive controls are identical to those used in Figure S2. (A) Histograms show % $CD4^+CD69^+$ and % $CD4^+CD25^+$. (B) Quantification of histograms are shown in A.

Figure S4. Effects of TAT-G-Gpep on $CD4^+$ and $CD8^+$ T-cells of human PBMCs. (A, B) Freshly isolated human PBMCs were labeled with CFSE and cultured for 3 days on anti-CD3 antibody coated plates with either TAT-G-Gpep-Sc or TAT-G-Gpep. Cells were collected and stained with CD4 and CD8 antibodies. Negative control: no anti-CD3, no peptide; positive control: anti-CD3, no peptide. (C, D) CFSE-labeled human PBMCs were cultured with anti-CD3 as in (A, B) with various concentrations of IFN-β. Negative control: no anti-CD3, no IFN-β; positive control: anti-CD3, no IFN-β.

Figure S5. Lack of effects on basal synaptic transmission by TAT-G-Gpep peptide. Hippocampal slices were prepared from TAT-G-Gpep or TAT-G-Gpep-sc control peptide-injected mice and evoked synaptic responses were recorded in the CA1 region of the hippocampus using a range of stimulation intensities. (A) fEPSP slopes as a function of stimulation intensities showing no differences between the TAT-G-Gpep and TAT-G-Gpep-sc control peptide-injected animals. (B) Prefiber volley as a function of stimulation intensities showing no differences between TAT-G-Gpep and control peptide-injected animals. (C) fEPSP slopes as a function of prefiber volley showing similar responses between the TAT-G-Gpep and control peptide-injected animals.

Video S1. EAE mice displayed significant hind limb paralysis after 10 days of MOG immunization. However, this motor dysfunction was drastically improved with daily administration of TAT-G-Gpep (i.p.) from day 10 to day 28.

